Journal of Computational Applied Mechanics 2021, 52(4): 664-681
DOI: 10.22059/jcamech.2021.333705.662

RESEARCH PAPER

Analyses of entropy generation for a solar minichannel flat plate collector system using different types of nanofluids

Lakhdar Bouragbi[a,*], Azzouz Salaheddine[b], Brahim Mahfoud[c]

[a,b]*Mechanical Laboratory of Materials and Industrial Maintenance (LR3MI), Badji Mokhtar University, Annaba, Algeria.*
[c]*Department of Mechanical, University of UAMO-Bouira, 10000, Algeria*

Abstract

The working fluid plays a major role in improving the efficiency of the energy system, so the method and criteria of choice are extremely important. Nevertheless, these methods are usually based on the First Law of Thermodynamics (FLT), while the concepts of entropy and irreversibility on which the Second Law of Thermodynamics (SLT) is based are often ignored in the choice of the fluid. In this paper, a new approach is proposed to select a fluid among a group of fluids in order to use it as a working fluid in a Minichannel Flat Plate Solar Collector (MFPSC). For this, a numerical simulation was performed on a fluid in laminar flow in a small rectangular channel subjected to a uniform heat flux of (1000 W/m^2). The use of Computational Fluid Dynamics (CFD) based on the finite volume method was implemented to solve the governing equations. The essential parameters on which the selection is based are the entropy generation (Sgen), the irreversibility of entropy generation number (Ns), the Bejan number (Be), and the Energy Performance Criterion (EPC). The analyses were performed on a group of five fluids two conventional (water and methanol), the rest are nanofluids (Al_2O_3-H_2O, CuO-H_2O, and Fe_3O_4 -H_2O). Multiple parallel-computation phases are defined by user-defined functions (UDFs) for all fluids. It is found that nanofluids offer higher heat transfer ability than conventional fluids, and the behavior of the nanofluid (CuO-H_2O) shows on average a minimum total entropy generation (minimum irreversibility) compared to other fluids (conventional and nanofluids), which reduces the energy degradation and improves the heat transfer. Therefore, it is chosen as the working fluid for the MFPSC.

Keywords: Collector, entropy generation; irreversibility; minichannel, nanofluid

1. Introduction

Rationalizing energy consumption and shifting to renewable energy are now clearly two compelling strategies in the policy-making of most countries in the world, given the growing danger of climate change due to carbon dioxide (CO_2), emissions, the principal source of global warming resulting from the increasing consumption of fossil energy sources. Solar energy with its two components (solar thermal and solar photovoltaic) is one of the most promising energy sources in the world. Nevertheless, its efficient conversion into a usable form remains an active research topic for scientists [1].

* Corresponding Author Email:Bouragbilakhdar@gmail.com

Solar systems used to heat fluids (liquid or gas) in the industrial or domestic field are important in many solar thermal sector applications. The solar collector is considered the key element of these systems, as it is the main component responsible for converting the energy of the solar radiation into heat and transferring it to the fluid to be heated directly or to a working fluid. Furthermore, this heat can then be stored or used directly [2].

Solar water heaters, especially flat plate solar collectors (FPSC), are largely used in most countries worldwide. They are mostly installed on the roofs of residential buildings. Research on solar thermal systems focuses on improving the energy performance of these components (FPSC) and, in particular, increasing conversion efficiency.

To make these solar collectors more energy-efficient and less expensive, the researchers' efforts focused on three directions. The first, indoor/outdoor design and construction materials, where the various designs of solar collectors, including solar water heaters, have been extensively studied and analyzed by many researchers, and there are many references in this research area [3- 6]. The second, the working fluid to be used in the solar collector. The research in this area has not been limited to conventional fluids but has led to other areas such as nanofluids and hybrid nanofluids; one can look at the current research and developments in these review articles, [7-13]. Finally the concepts, theories, and methods of study as well as analysis and design tools that continue to increase and expand, especially with the development of programming languages and numerical simulation codes (CFD: Computational Fluid Dynamics), as well as the storage capacity and speed of computers to perform calculations, in order to clarify some trends for this aspect, here are some References [14-17].

In this paper, we mainly aim to compare the energetic behavior of five fluids to classify them and choose the best fluid to be used as a working fluid in a solar water heater to improve the thermal efficiency of the solar collector. It has been observed that theoretical or experimental studies of comparison and selection of working fluids. However, they offer new methods, have often been based on the first law of thermodynamics(FLT), and thus neglect the energy degradation due to the irreversibility phenomenon that expresses entropy generation, a concept that the second law of thermodynamics (SLT) is based on.

Since the publication of Adrian bejan [18], the number of publications in this field has multiplied, and a recent field has emerged, called Entropy Generation Minimization (EGM) or irreversibility minimization. In this work, the main idea on which we are based in the search for a working fluid that behaves with minimal entropy generation; we perform a three-dimensional simulation of the flowing fluid with data from a real model of a rectangular cross-section minichannel solar water heater, built for experimental and study purposes by Duong [19], which is detailed in her thesis.

We took pure water and methanol for the studied fluids, which are well known in solar energy applications, especially in heat pipes. Thus, Taoufik *et al*. [20].studied the impact of these two fluids on the performance of a solar collector using a screen mesh heat pipe. They found that water is better than methanol, where the instantaneous efficiency of the collector is close to 60%. However, this study was only based on the FLT, which ignores the behavior of the fluid towards irreversibility, and the results may be different if the concept of entropy generation (i.e., SLT) is introduced.

For this purpose, we added to these two conventional fluids (water and methanol) three other nanofluids (water-Al_2O_3, water-CuO, and water-Fe_3O_4), which are also known for their excellent heat transfer properties. Nanofluid is a new kind of heat transfer medium. However, the influence of several parameters, such as size and shape, phenomena at the interfaces between the liquid and the particles, which are still poorly understood and distinguished is still

being researched and experimented [21], we will not address them in this paper, but we consider them as fixed in the properties, as will be clarified in paragraph (§ 2.5).

The behavior of these three water-based nanofluids (Al_2O_3, CuO, and Fe_3O_4) towards heat transfer by convection has been studied by Golkonda and Srinivasa [22]. However, their study was done only under turbulent flow conditions and without introducing the concept of entropy generation, which is more apparent due to the turbulence of the fluid during its motion. We also refer to another numerical study of these three nanofluids carried out by Arani1 *et al*. [23], which also analyses their energetic behavior. However, the geometry is different from ours; we record that if they included the concept of entropy generation in their investigation, the results would have been richer.

In the present paper, we propose an alternative approach for selecting one of a group of fluids to be used as a working fluid in a minichannel flat plate solar collector (MFPSC).

For this purpose, we use the Computational Fluid Dynamics (CFD) based on the finite volume method, a numerical simulation has been performed for each fluid in laminar flow inside a minichannel with a rectangular section and a uniform heat flux of (1000 W/m^2) applied to its upper surface. The main parameters on which the selection method is based are the entropy generation (Sgen), the irreversibility of entropy generation number (Ns), the Bejan number (Be) and the energy performance criterion (EPC). As for the validation, it is done mainly using the Nusselte number

2. Mathematical Modeling

2.1 Model

We consider a solar flat plate collector (MFPSC) with rectangular minichannel as shown in Fig.1. The nomenclature of the solar MFPSC used in the current work is taken from a study of Duong and Sai *et al*. [19,24] The minichannel channel tubes are made of copper, which the copper MFPSC has shown promising results using for medium temperature process heating applications. The internal dimension of channel width is 2.5mm, channel height is 2mm and the channel length is 300mm, and plate thickness (E_h= 0.3, E_v=0.15). A constant heat flux (1000W/m2) is applied at the outside of the top wall of the minichannel outside of the top wall of the minichannel (Table.1). The working fluids and nanofluids used in the simulation are pure water, methanol, Al_2O_3-H_2O, CuO-H_2O, and Fe_3O_4-H_2O, respectively.

The steady-state flow is supposed to be laminar, and incompressible. The inlet velocity=0.04m/s is axially imposed and the temperature is 300k in the entrance of the minichannel. A conjugate heat transfer from the outer wall to the fluid is considered, which combines thermal conduction in the solid wall and convective heat transfer from the inner surface to the fluid.

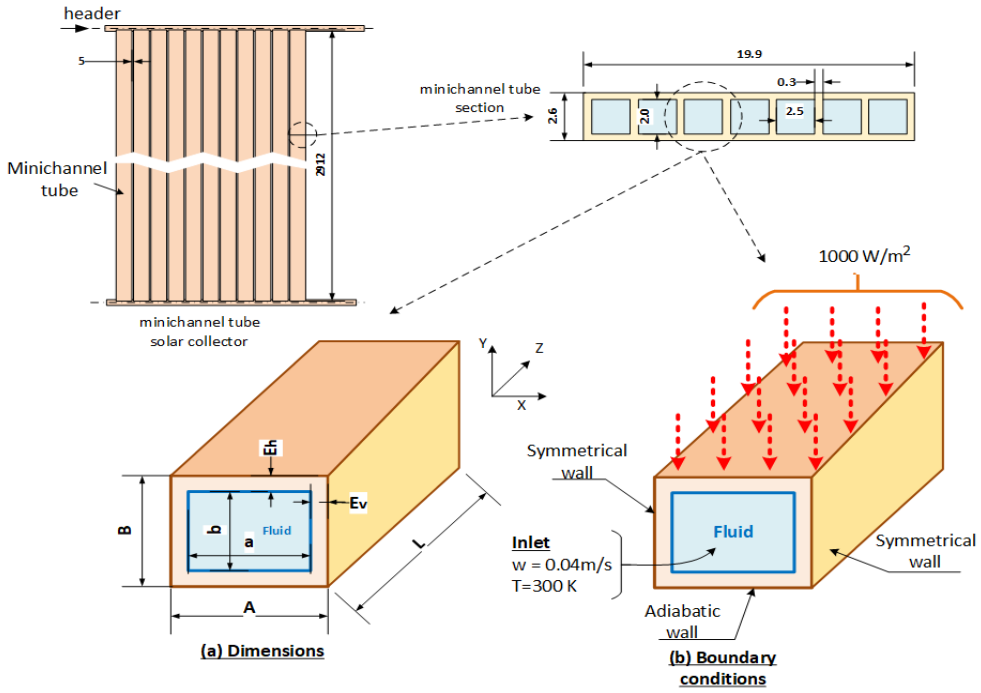

Figure 1. Illustration drawings of the computational domain for a single rectangular minichannel. (a) Dimensions of the minichannel (b) Boundary conditions applied to the computational domain. for thermal analysis

Table 1. Dimensions of single rectangular minichannel

Parameters	*a*	*b*	*A*	*B*	*L*	*Ev*	*Eh*
Values(mm)	2.5	2	2.8	2.6	300	0.15	0.3

2.2 *Governing Equations*

The following assumptions are given to simplify the mathematical modeling: (i) the fluid flow is laminar and the heat transfer occurs at a steady-state, (ii) all fluids considered here are incompressible and Newtonian, (iii) The temperature of the air between plate and glass cover is uniform (iv) properties of fluids are constants and appraised at the reference temperature, (v) Viscous dissipation terms are neglected, (vi) The conductive heat transfer along the length of the channel (axial direction) is considered, (vii) Plate material properties do not vary due to changes in plate temperature.

Based on the above assumptions, the considered flow can be controlled by the continuity, momentum, and energy equations widely detailed in the heat transfer and fluid mechanics literature. For more details, one can see [25,26] These equations can be expressed as:

✓ *Continuity equation:*

$$\frac{\partial u}{\partial x}+\frac{\partial v}{\partial y}+\frac{\partial w}{\partial z}=0 \tag{1}$$

✓ *X-momentum equation:*

$$\rho\left(u\frac{\partial u}{\partial x}+v\frac{\partial u}{\partial y}+w\frac{\partial u}{\partial z}\right)=\frac{\partial P}{\partial x}+\mu\left(\frac{\partial^2 u}{\partial x^2}+\frac{\partial^2 u}{\partial y^2}+\frac{\partial^2 u}{\partial z^2}\right) \tag{2}$$

✓ *Y-momentum equation:*

$$\rho\left(u\frac{\partial v}{\partial x}+v\frac{\partial v}{\partial y}+w\frac{\partial v}{\partial z}\right)=\frac{\partial P}{\partial y}+\mu\left(\frac{\partial^2 v}{\partial x^2}+\frac{\partial^2 v}{\partial y^2}+\frac{\partial^2 v}{\partial z^2}\right) \quad (3)$$

✓ *Z-momentum equation:*

$$\rho\left(u\frac{\partial w}{\partial x}+v\frac{\partial w}{\partial y}+w\frac{\partial w}{\partial z}\right)=\frac{\partial P}{\partial z}+\mu\left(\frac{\partial^2 w}{\partial x^2}+\frac{\partial^2 w}{\partial y^2}+\frac{\partial^2 w}{\partial z^2}\right) \quad (4)$$

✓ *Energy equation*

$$\rho C_p\left(u\frac{\partial T}{\partial x}+v\frac{\partial T}{\partial y}+w\frac{\partial T}{\partial z}\right)=+k\left(\frac{\partial^2 T}{\partial x^2}+\frac{\partial^2 T}{\partial y^2}+\frac{\partial^2 T}{\partial z^2}\right) \quad (6)$$

2.3 *Entropy Generation*

In the following, we present the definition of S_{gen} entropy generation in a system, but we only write the crucial relations used in our calculations, and anyone who wants to know more can refer to [27,28,29]. According to Bijan. [25], for a control volume of finite size x y z at an arbitrary point (x, y, z) in a flow field, the entropy generation rate per unit time and unit volume is :

$$\dot{S}'''_{gen}=\dot{S}'''_{gen,h}+\dot{S}'''_{gen,f}\geq 0 \quad (7)$$

Where $\dot{S}'''_{gen,h}$ and$\dot{S}'''_{gen,f}$ are the 3D volumetric thermal and viscous entropy generation rates, respectively, and are expressed as:

$$\dot{S}'''_{gen,h}=\frac{k}{T^2}\left(\left(\frac{\partial T}{\partial x}\right)^2+\left(\frac{\partial T}{\partial y}\right)^2+\left(\frac{\partial T}{\partial z}\right)^2\right) \quad (8)$$

$$\dot{S}'''_{gen,f}=\frac{\mu}{T}\left[2\left(\left(\frac{\partial u}{\partial x}\right)^2+\left(\frac{\partial v}{\partial y}\right)^2+\left(\frac{\partial w}{\partial z}\right)^2\right)+\left(\frac{\partial u}{\partial y}+\frac{\partial v}{\partial x}\right)^2+\left(\frac{\partial u}{\partial z}+\frac{\partial w}{\partial x}\right)^2+\left(\frac{\partial w}{\partial y}+\frac{\partial v}{\partial z}\right)^2\right] \quad (9)$$

Where k and μ are the fluid's thermal conductivity and dynamic viscosity, respectively, which are assumed to be constant, Trepresents the reference temperature taken equal to the inlet temperature of the fluid T_{in}.

The global entropy generation rate is determined using the volumetric entropy generation over the full domain. The equation is linked as follows:

$$\dot{S}_{gen}=\iiint_{\Omega}\ S'''_{gen}\,d\Omega \quad (10)$$

Where Ω represents the computing volume.

2.3.1 *Bejan Number*

Bejan number Be was recently introduced by Paoletti *et al.* [30] and Benedetti and Sciubba[31]. It is an alternative distribution fraction of the irreversibility. It is the ratio between the entropy generation from heat transfer and the total entropy generation. It is written as follows:

$$Be = \frac{\dot{S}'''_{gen,h}}{\dot{S}'''_{gen,h}+\dot{S}'''_{gen,f}} \quad (11)$$

2.3.2. *Entropy Generation Numbers*

The dimensionless entropy generation number (Ns) is defined as the global entropy generation $\dot{S}'''_{gen}$ divided by the heat capacity rate $\dot{m}C_p = \dot{Q}/T_{in}$ of the fluid. It also represents irreversibility.

$$N_s = \frac{\dot{S}'''_{gen}}{\dot{Q}/T} \quad (12)$$

Where $\dot{Q}$ is the heat transfer rate, and T is the reference temperature that is assumed to be equal to the inlet temperature of the fluid.

2.3.3. *Energy Performance Criterion (EPC)*

This factor represents the ratio between the thermal power exchanged with the fluid and the pumping power required to pass through the heat exchange between the outlet and inlet temperatures of the fluid (T_{out}, T_{in}) [20],commonly called the Energy Performance Criterion (EPC):

$$EPC = \frac{\dot{m}C_p(T_{out}-T_{in})}{\dot{V}\Delta P} \quad (13)$$

Where $\dot{m}(Kg/s)$, $\Delta P(Pa)$ represent mass flow rate, volume flow rate, and pressure drop.

2.4. *Thermophysical Properties of Fluid*

The nanofluid is a new type of heat transfer fluid consisting of stable and uniformly distributed nanoparticles of different shapes, ranging in size from 1 to 100 nm, suspended in a base fluid such as pure water or another solution. In this work, five fluids are chosen for the comparative study in a liquid state under normal conditions. These fluids can be used as working fluid in flat plate solar collectors. Two of them are ordinary conventional liquids: pure water and methanol. As for the other three liquids, they are so-called nanofluids, in the composition of which pure water is used as a primary element with the addition of a specific percentage of mineral particles to improve its properties and thermal performance, namely: (Al_2O_3 + H_2O), (Fe_3O_4 + H_2O) and (CuO + H_2O).

The fluids have physical properties assumed constant with temperature such as $\left(\rho_{nf},\ \mu_{nf},\ C_{p_{nf}},\ k_{nf}\right)$, these parameters are obtained from the property tables but for the others, it depends on the volume fraction φ of the solid particles in the suspension and the shape of the particles added in pure water. In this paper, we took $\varphi = 0.5\%$ for Al_2O_3 studied in[32],$\varphi = 0.15\%$ for CuO studied in [33], and $\varphi = 0.8\%$ Fe_3O_4 studied by Saidu *et al*.[34]. Thermophysical properties at temperature T=300 K are given in Table 3, they are calculated from equations (14-17) using the values in Table 2.

- *Thermal conductivity*

$$k_{nf} = \left(\frac{k_p+(n+1)k_f-(n-1)\varphi(k_{bf}-k_p)}{k_p+(n-1)k_{bf}+\varphi(k_{bf}-k_p)}\right)k_{bf} \quad (14)$$

Where n is the solid particle shape factor (n = 3 for spherical particles assumption).

- *Dynamic viscosity*

$$\mu_{nf} = \mu_{bf}(1 + 2.5\varphi) \quad (15)$$

- *Density*

$$\rho_{nf} = (1-\varphi)\rho_{bf} + \varphi\rho_p \quad (16)$$

- *Heat capacity*

$$c_{P_{nf}} = (1-\varphi)c_{Pnf} + \varphi c_{P_P} \quad (17)$$

where φ represents the volume fraction of the mineral particles, the subscripts $\ll nf, bf,$ and $p \gg$ are for the nanofluid, the base fluid (pure water), and the particle, respectively.

The flow rate, volume fraction, and particle size strongly influence the thermal conductivity of nanofluids [35]. To avoid their effect, in this study, we took these parameters as constant. All properties at temperature $T = 300°C$ are grouped in Tables(2-3).

- ***Boundary Conditions***

As illustrated in Figure 1 b, the applied boundary conditions are defined as follows:
At the inlet of the minichannel, we get uniform velocity and temperature profiles at which:

$$u = v = 0\,, w = w_{in} = 0.04\,m/s\,, \text{and T} = T_{in} = 300k \quad (18)$$

A constant uniform heat flow is applied to the upper external surface of the minichannel, where $q_w = 1000\,W/m^2$

Pressure gradients at the outlet of the minichannel equal to zero

$$q_w = -k_s \frac{\partial T_s}{\partial y} \quad (19)$$

The two vertical wall surfaces (left/right) of the calculation domain (Figure 1) are defined as symmetry, i.e., no diffusion flux takes place through the symmetry surfaces.

$$-k_s \frac{\partial T_{sv}}{\partial y} = 0 \quad (20)$$

The bottom surface is defined as an adiabatic wall.

Inside the minichannel, the solid/fluid interface is defined as a wall to couple fluid convection and solid conduction, and the velocity components are zero:

$$u = v = w = 0;\; T_s = T_f;\; -k_s \frac{\partial T_s}{\partial n} = -k_f \frac{\partial T_f}{\partial n} \quad (21)$$

Table 2. Thermophysical properties of Al_2O_3, CuO, and Fe_3O_4 at T=300 K[36-39].

Material	Thermal conductivity $k(W/m.K)$	Density $\rho(Kg/m^3)$	Heat capacity $C_p(J/Kg.K)$
Al_2O_3	36	3600	765
CuO	76.5	6400	531
Fe_3O_4	17.65	5180	104

Table 3. Thermophysical properties at temperature T=300 K of the studied fluids.

Fluids	Volume fraction $\varphi(\%)$	Thermal conductivity $k(W/m.K)$	Dynamic viscosity $\mu(Kg/m.s)$	Density $\rho(K/m^3)$	Heat capacity $C_p(J/Kg.K)$
Water (H_2O)	-	0.613	0.001003	996.5	4181.2
Methanol (CH_3OH)	-	0.1982	0.0005280	784.8	2561,00
Al_2O_3-H_2O	0.05	0.710	0.00112838	1146.79	4009.44
CuO-H_2O	0.05	0.702	0.00112838	1268.29	3997.74
Fe_3O_4-H_2O	0.8	0.781	0.0012036	1332.744	3854.10

3 Numerical Procedure, Grid Test and validation

3.1 Numerical procedures

In this study, the OpenFOAM software, which is based on the finite volume method [41], is used in all simulations. The SIMPLE algorithm [42] is chosen to allow the pressure-velocity coupling. Momentum and energy equations are approximated with a second-order difference scheme. The solution is considered convergent when the values of the residual criteria attain 10^{-6} for all variables. And then, the solution datasets are loaded directly into CFD-Post to be processed and examined to extract the relevant model observations for discussion. Regarding the generated entropy represented by equations (7, 8, 9, and 10), we can evaluate velocity and temperature fields from a CFD calculation to know all the mean velocity and temperature gradients for the problem. Therefore, the entropy generation rate for each fluid can be calculated in a post-processing procedure.

3.2 *Grid Independence Test*

Taking into account that the aspect ratio (L/a =120), a careful choice of the grid is needed to ensure good accuracy. A mesh with quadratic elements was selected; the details of grid independence tests are shown in Table 4. The influence of the number of control volumes on the precision of the results was studied, where the average Nusselt number through the top wall average temperature in function of number of control volume in the computational domain is represented. As we increase the number of control volumes above 7338552 the average Nusselt number becomes almost constant. Consequently, the grid of 7338552 nodes has been used in all calculations of this study.

Table 4 . Grid independence test

Nodes	Av-Nu	T_m (at z=0.15 and
6018231	4.14	300.14
6526542	4.26	300.19
7033495	4.30	300.25
7213232	4.33	300.301
7338552	4.36	300.302
7439360	4.36	300.302

3.3 *Validation*

First, these results obtained are validated with the results found in the literature. Fig.2 shows the temperature profiles of the fluid at the center wall, the inner and outside wall. It can be seen that the temperature curves of the fluid at the center of the minichannel and that of the wall are parallel in the region where the flow is fully developed (from z=0.075mm); this is in good accord with the literature in the domain of heat transfer for a heated fluid flows in a pipe by a constant uniform heat flow applied to its external surface (see page 426 of reference [25].
Secondly, the simulation results are validated by evaluating and plotting the average Nusselt number Nu as a function of the z distance compared to those performed by Shah and London [40]. The equation of the average Nusselt number used for the validation is given by:

$$Nu = \frac{\dot{q}'' d_h}{k_f (T_w - T_m)} \tag{22}$$

Where T_w is the average temperature at the boundary; it represents the internal temperature of the heated wall. $T_m$is the mean temperature, for incompressible flow in a minichannel with an equivalent hydraulic radius $(R = d_h/2)$ the expression of $T_m$is given by:

$$T_m = \frac{\int_{r=0}^{R} Twrdr}{\int_{r=0}^{R} wrdr} \tag{23}$$

The average Nusselt number that is given in[36] has a constant curve *Nu*=4.36, which is given by the classical empirical solution. In contrast, the average Nusselt number calculated by CFD presents high values at the inlet in the area where z< 0.075m, this difference is due to the velocity applied at the inlet being constant, and uniform in the current study (V = 0. 04m/s) are profile stabilizes from the area defined by z>0.075 where the flow becomes fully developed. The two curves coincide well in this region, which means the excellent agreement between the simulation results and experimental data given in [40].

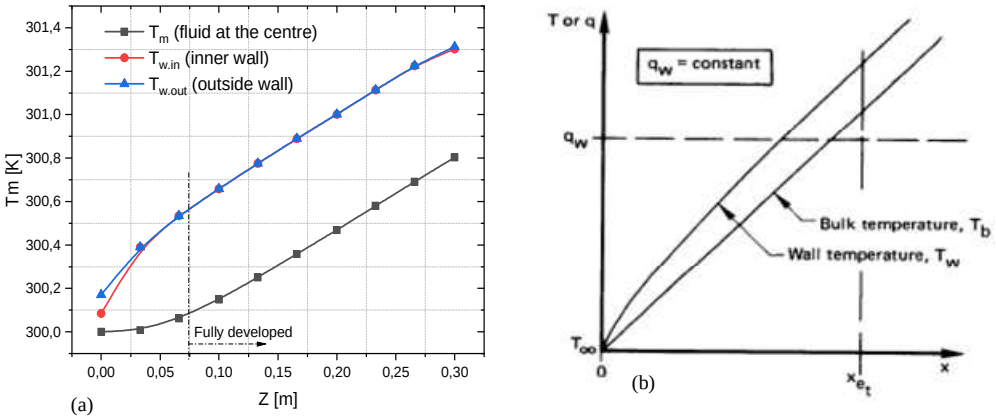

Figure 2. Variation of the mean temperature along the duct with uniform heat flux comparison between (*a*) present work and (b) [25] (see page 426).

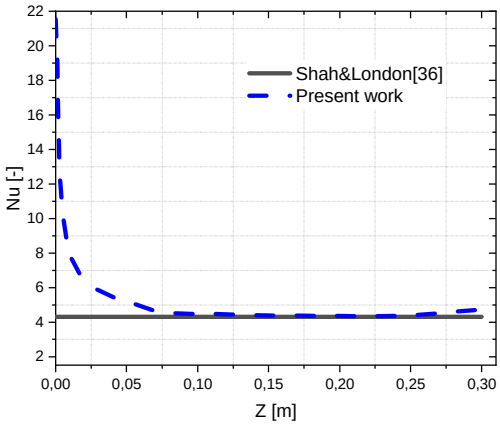

Figure 3. Average Nusselt number vs Z- distance

3. Results and discussions

For all simulations, the heat flux is fixed at 1000W/m^2, the inlet temperature is T=300K. Although solar irradiation was a driving factor for collector performance, it was also found that fluid inlet temperature also held a very high significance. In this context, the influence of nanofluid on the increase of the outlet temperature will be examined. Therefore the entropy generation, the minimum irreversibility, the energy performance, and the convection heat transfer using for analysis. The analyses were done for several nanofluids and then compared with methanol and pure water. Commonly, the performance of MFPSC is ascertained based on two performance measures, collector efficiency, and fluid outlet temperature. By regarding Fig. 4a, which presents the contours of isotherms at different plans along the direction (oz-axis) of the fluid flow for the case of CuO nanofluid (Results are similar for other fluids), it is noticed that the temperature at the outer increase with increasing z-distance of the minichannel.

The variation of the average Nusselt number with z-distance is presented in Fig. 4b, where pure water, methanol, and other nanofluids are compared. It can be seen that *Nu* monotonically decreases with an increase in z and approaches to the value of the conduction limit. We observe that all the studied fluids (conventional or nanofluid) have the same behavior whether in the fully developed zone or before this zone However, the lighter hot fluid near the walls of the minichannel surrounds the cold fluid which concentrates in the middle of the minichannel. It is observed that at a fixed z-distance, the value of *Nu* for methanol is greater than those obtained in the cases of pure water and nanofluids. We conclude that the use of methanol results in more improvement in heat transfer compared to other fluids and nanofluids, but uncertain that it is a feasible fluid for maximum performance, which will be discussed in detail in the next section.

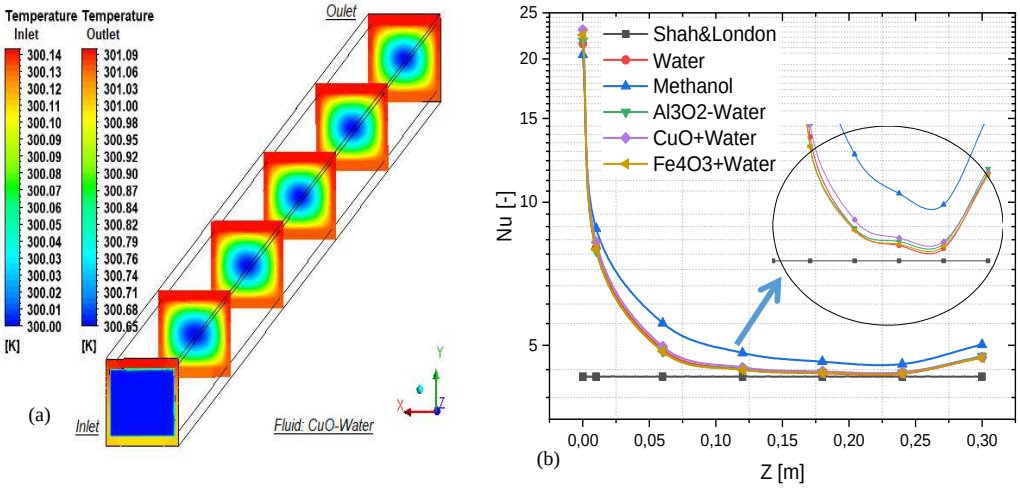

Figure 4 (a) isotherms in different plan (b) comparison of average Nusselt number for several nanofluids

4.1 *Energy Performance Criterion (EPC)*

Figure 5. illustrates a comparison of the number of PCEs obtained from the relation (13) for the concerned fluids, where the calculation results are developed in (Table 4). It is clear that the bar of methanol is the highest, it reaches a value of EPC equal to 90574.72, this means that the thermal power transferred by methanol along the minichannels is the most important both the pumping power and the lowest. This is due to its low density784.8 Kg/m^3, which is the lowest among the other liquids. On the other hand, we find that the Fe3O4-H2O nanofluid records the lowest EPC value, which is also due to its high density, the reason why they are considered as reference points for the calculation of the percentage of the PCE increase. We also observe that the pressure drop and pumping power of methanol are four times lower than that of water and more than 16 times lower than that of nanofluids (Al_3O_2-Water and CuO+Water). The specific heat values of water and nanofluids are very close and higher (by about 1.5) than that of methanol, although the influence of density is dominant than the fluid's ability to heat. we conclude in this paragraph that methanol is the best candidate to be the working fluid. But it should be noted here that a selection based only on PEC is an incomplete selection, because it is based only on SLT, and does not show us which system (Fluid+ Minichannel) degrades the most energy, or where or how, because it is concerned with balance and conservation of energy and neglects the point of view of energy degradation known as irreversibility or entropy generation on which the SLT is based, which will be discussed in more detail in the following paragraphs.

Table 5. Histogram of the number of energy performance criterion EPC of fluids

Fluids	ρ (Kg/m^3)	C_p ($J/Kg.K$)	T_{out} (°C)	ΔT (°C)	ΔP (Pa)	EPC	% (*)
Water (H_2O)	996.5	4181.2	300.915	0.915	72.0	52950.11	20.14
Methanol (CH_3OH)	784.8	2561,00	301.84	1.84	40.83	90574.72	**100.00**
Al_2O_3-H_2O (f=0.05)	1146.79	4009.44	300.837	0.837	82.5	46648.65	6.76
CuO-H_2O (f=0.05)	1268.29	3997.74	300.751	0.751	83.2	45766.71	4.89
Fe_3O_4-H_2O (f=0.8)	1332.744	3854.10	300.748	0.748	88.4	43462.93	**0.00**

(*)The percentage values in the last column are calculated in relation to the increase between the min and max PEC values (i.e.: $\Delta PEC = PEC_{max} - PEC_{min}$, $and\ \% = (PEC - PEC_{min}) * 100/\Delta PEC$).

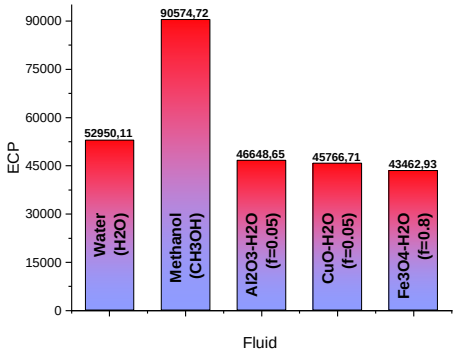

Figure 5. Comparison between the EPC number's

4.2 *Entropy Generation*

In Fig.6(a) it appears that methanol presents a minimum of entropy generation S_{gf} due to friction forces, which shows an agreement with the previous observation of the low EPC number of pressure losses compared to other fluids. However, the entropy generation due to heat transfer presents maximum S_{gh}(Fig.6b) . That is to say, the thermal behavior of methanol presents the maximum irreversibility (maximum energy degradation), which makes its choice as a working fluid very unlikely. As for the other fluids, we also observe that the nanofluids (Al_2O_3-H_2O and CuO-H_2O) present a very similar behavior and are globally positioned in middle-order in terms of entropy generation.

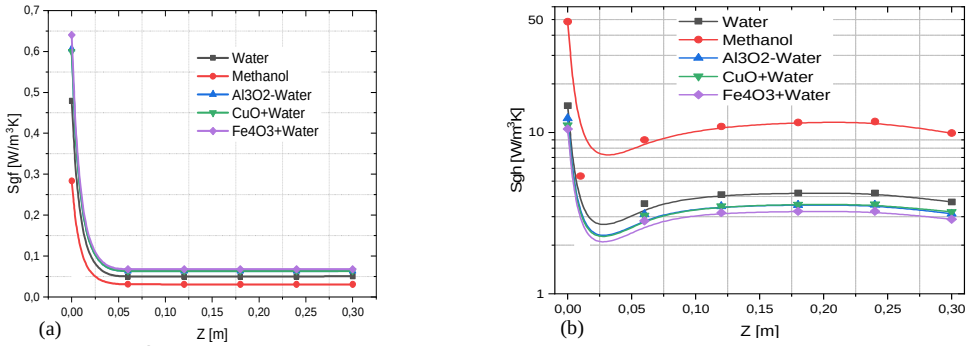

Figure 6. Variation of (a)local viscous entropy generation rate and (b) thermal entropy generation rate Vs z-distance.

It is also noted that the values of the entropy generation by the heat transfer S_{gh} is higher about 16 times compared to that of the entropy generation due to the frictional forces S_{gf} (i.e., $S_{gh} \cong 16S_{gf}$), the reason for which the curves of the total entropy generation S_g coincide much with that of S_{gh} as shown in Fig 7(a). This figure also shows that nanofluids present almost constant local entropy generation values with distance and less than conventional fluids.

However, in Fig. 7(b), the total volumetric entropy generation increases with the fluid volume along the minichannel's length. Nevertheless, the superposition of the two nanofluids (Al_2O_3-H_2O and CuO-H_2O) previously noted persists. On the other hand, the curve for the nanofluid (Fe_3O_4-H_2O) shows that it moves away a bit downward, forming a decrease in volumetric entropy generation as a function of volume increase along the length of the minichannel. Therefore, this nanofluid (Fe_3O_4-H_2O) becomes the candidate to be the working fluid instead of methanol.

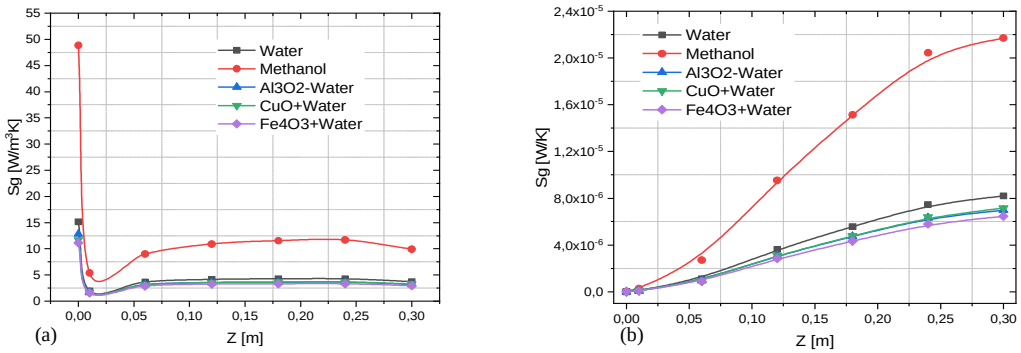

Figure 7. Change of local total (a) entropy generation $S_g[W/m^3K]$with distance, (b)volumetric entropy generation Sg [W/K] with distance

4.3 Bejan Number

The Fig. 8 shows the variation of the Bejan number Be as a function of the distance (z) covered by the fluid inside the minichannel. The Bejan number expressed by the equation (11) also allows us to see which mode of irreversibility or entropy generation $(S'''_{gen.h},\ S'''_{gen.f})$ is moreover manifested for each flow of the fluid.

Starting from the region where the fluid is fully developed, we observe that all fluids have curves of Be = f(z) more significant than the average Bejan number Be=1/2 which means that irreversibilities due to heat transfer are in the majority, this may be caused by the amount of heat of 1000W/m^2 applied to the external surface of the minichannel. Moreover, methanol presents values very close to unity (Be=1), which means that the irreversibility due to heat transfer dominates and that the irreversibility due to viscous force is negligible. On the other hand, the nanofluid (Fe_3O4-H_2O) presents irreversibility due to the viscous force that can be high, which leads to a degradation of energy and make the pumping power higher compared to the other fluids.

This may be due to the density of the nanofluid (Fe_3O_4-H_2O) being the highest (1332.744 kg/m3) and conversely that of the conventional fluid methanol being the lowest (784.8kg/m3), but the density of the (Fe_3O_4-H_2O) comes down to two factors: the geometry of the iron particles and the fraction of these particles suspended in the water (f=0.8). This is an issue that requires further research, which we cannot address here.

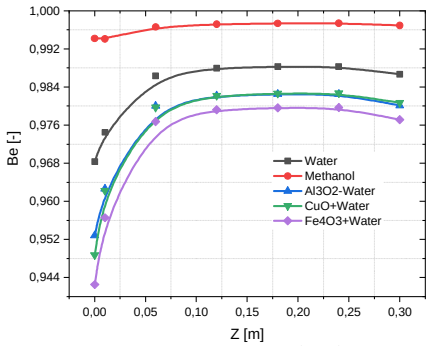

Figure 8. Change of bejan number (Be) vs z- distance.

Fig.9 displays the evolution of the entropy generation number calculated from the relation (12). Here it is clear for the two conventional fluids that they have different and divergent behavior, for methanol the number of entropy generation N_s increases with the increase of the volume of the fluid, that is to say, with the length of the minichannel, on the other hand, pure water has almost constant values, especially in the region where the flow is fully developed, its average value is about 2×10^{-12}.

As for the Al_3O_2-Water nanofluids, N_s number increases with the minichannel length, but their curves coincide for the other two nanofluids Fe_3O_4-H_2O and CuO-H_2O. They present a similar behavior and are close to the behavior of water, which favors the use of nanofluids as a working fluid, especially when there is a possibility of controlling and adapting their physicochemical properties. From these results, it can be seen that CuO-Water nanofluid is the best candidate for working fluid in the minichannel solar collector.

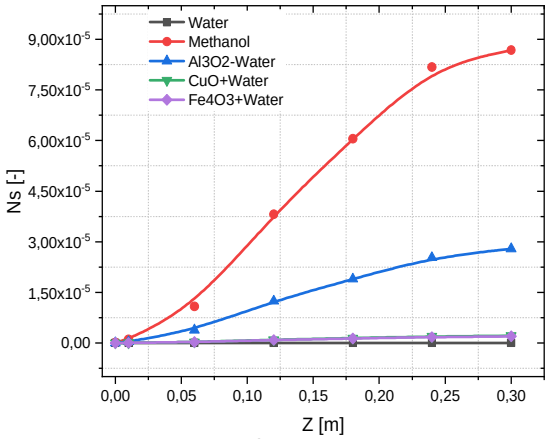

Figure 9. Change of entropy generation number

5. Conclusion

This paper has used a numerical simulation to analyze and predict the performance of a solar minichannel flat plate collector. Five fluids, including three water-based nanofluids (Al_2O_3 and CuO and Fe_3O_4) and two conventional, pure water and methanol have been performed. The numerical estimation in three dimensions of the entropy generation of these fluids circulating in a heated rectangular minichannel, numerical analysis, and comparison of their thermal behaviors are performed. The main conclusions are the following:

✓ In minichannel solar collectors (liquid without phase change), pure water-based nanofluids show remarkable convective heat transfer rate improvement. They seem to be the best replacement for conventional pure fluids.

✓ The classification by order of preference of the studied fluids that we have obtained through this discussion is the following: CuO-H_2O, Fe_3O_4-H_2O, Al_3O_2-Water, pure water, Methanol. Therefore, CuO-Water nanofluid is the best candidate for working fluid in the minichannel solar collector.

✓ The behavior of methanol in the minichannel shows the highest rate of entropy generation due to heat transfer (S_{gh}) compared to other fluids, while the rate of entropy generation due to frictional force (S_{gf}) is the lowest. This shows that it is preferable to use it in the low-temperature range (cooling system) and does not require considerable pumping power or in the heat pipe area with thermosiphon circulation.

✓ It appeared that classification or selection of the fluid based on parameters and expressions obtained from the first law of thermodynamics is insufficient because the degradation of energy by entropy generation (irreversibility) has not been taken into account,

so the SLT must be introduced to evaluate and show the types of energy waste by entropy generation.

Nomenclature

d_h Hydraulic diameter *(m)*	Ω Computing volume
u, v, w Velocity (m/s)	Nu Nusselt number
$\dot{m}$ Mass flow rate	Be Bejan number
$\dot{V}$ Volume flow rate (m^3/s)	N_s Creation entropy number
ρ Density $(Kg/m^3.)$	EPC Energy Performance Criterion
μ Dynamic viscosity $(Kg/m.s)$	
C_p Heat capacity $(J/Kg.K)$	*Indices*
ΔP Pressure drop (Pa).	gen Entropy generation rates
k Thermal conductivity $(W/m.K)$	gen, h Thermal entropy generation rates
T Temperature $(°K)$	gen, f Viscous entropy generation rates
$\dot{S}'''$ 3D volumetric entropy generation Rates$(W/m^3.°K)$	nf Nanofluid
Q Heat flow (W)	bf Base fluid (pure water)
q Density of heat flow (W/m^2)	p Particle
φ Volume fraction of the mineral particles (%),	in Inlet
	out Outlet
	w Wall

References

[1] João, P. C and B, Victor, M .(2016), CO2 emissions,non-renewable and renewable electricity production,economic growth, and international trade in Italy, Renewable and Sustainable Energy Reviews 55 (2016)142–155. http://dx.doi.org/10.1016/j.rser.2015.10.151

[2] Sadhishkumar, S and Balusamy, T.(2014), Performance improvement in solar water heating systems—A review", Renewable and Sustainable Energy Reviews, 37 (2014)191–198.

[3] Nurril, I. S. A. Hilmi, H. Shakir, M. N. and Tanweer, H.(2002), Thermal Performance Enhancement in Flat Plate Solar Collector Solar Water Heater: A Review, Processes 2020, 8, 756.doi:10.3390/pr8070756.

[4] Evangelisti, L. Roberto, D. L. V and Asdrubal, F. (2019), Latest advances on solar thermal collectors: A comprehensive review, Renewable and Sustainable Energy Reviews 114(2019)109318.https://doi.org/10.1016/j.rser.2019.109318

[5] Krishna, M. P and Rajesh, C. (2017), A review on analysis and development of solar flat plate collector, Renewable and Sustainable Energy Reviews.67(2017)641–650. http://dx.doi.org/10.1016/j.rser.2016.09.078

[6] Gianpiero, C. Ernani, F. Miglietta, P and Arturode Risi.(2016), Innovationin flat solar thermal collectors: A review of the last ten years experimental results, Renewable and Sustainable Energy Reviews 57(2016)1141–1159. http://dx.doi.org/10.1016/j.rser.2015.12.142

[7] Eric, C. Okonkwo, I. W. Ismail, W. Almanassra,Y. M. A. and Al□Ansari.T.(2020), An updated review of nanofluids in various heat transfer devices, Journal of Thermal Analysis and Calorimetry. published online :15 june 2020. https://doi.org/10.1007/s10973-020-09760-2

[8] Ifeoluwa, W. Eric; C. O. Abbasoglu, S and Doga, K. (2020), Nanofluids in Solar Thermal Collectors: Review and Limitations, International Journal of Thermophysics (2020) 41:157. https://doi.org/10.1007/s10765-020-02737-1

[9] Bhrant, K. D and Arvind K.(2019), A review on nanofluids for solar collector application, 3rd International Conference on "Advances in Power Generation from Renewable Energy Sources"2019.https://hq.ssrn.com/conference=2019-APGRES
[10] Ritvik, D. Prateek, N. Neeraj, S and Desh, B. S. (2019), A brief review on solar flat plate collector by incorporating the effect of nanofluid, Materials Today: Proceedings. https://doi.org/10.1016/j.matpr.2019.11.294
[11] Kadhim, A. H., Dong, L. Kolsic, L.Sanatana, K and Brundaban S.(2017) "A Review of Nano Fluid Role to Improve the Performance of the Heat pipe Solar Collectors ». Energy Procedia 109 (2017) 417 – 424.
[12] Mojtaba, N.(2016), Nano Fluid in Water as Base Fluid in Flat-Plate Solar Collectors with an Emphasis on Heat Transfe, .Indian Journal of Science and Technology**,** Vol 9(31), August 2016**.**DOI:10.17485/ijst/2016/v9i31/90341
[13] Lazarus, G. Raja, B. Mohan Lal, D and Wongwises, S.(2009), Enhancement of heat transfer using nanofluids—An overview, Renewable and Sustainable Energy Reviews 14 (2010) 629–641.doi:10.1016/j.rser.2009.10.004.
[14] Mahfoud, B. and Bendjaghlouli, A. (2018), Natural convection of a nanofluid in a conical container, Journal of Thermal Engineering (1), 1713–1723.
[15] Elumalai, V and Ramalingam, S.(2020), A review on recent development of thermal performance enhancement methods of flat plate solar water heater, Solar Energy 206 (2020) 935–961. https://doi.org/10.1016/j.solener.2020.06.059
[16] Nawaf, H. Waqar, K. Surafel, T.(2018), Optimization of Microchannel Heat Sinks Using Prey-Predator Algorithm and Artificial Neural Networks, Machines 2018, 6, 26.doi:10.3390/machines6020026
[17] Mohamed, M. A. (2015), A review of entropygeneration in microchannels, Advances in Mechanical Engineering. 2015, Vol. 7(12) 1–32. _ The Author(s) 2015. DOI: 10.1177/1687814015590297.
[18] Bejan, A. (1982), Entropy generation through heat and fluid flow, (John Wiley & Sons, Inc., New York).
[19] Duong,V. T (2015),,Minichannel tube solar thermal collectors for low to medium temperature application, Master of Science thesis, Mechanical Engineering Dept.,University of California, Merced. https://escholarship.org/uc/item/21r366cn. Publication Date 2015-01-01
[20] Taoufik, B. Dhaou, M. H and Abdelmajid, J. (2014), Theoretical and experimental investigation of plate screen mesh heat pipe solar collector , Energy Conversion and Management 87 (2014) 428–438 . http://dx.doi.org/10.1016/j. enconman.2014.07.041
[21] João, P.R. and Jean, A. G.(2009), Nanofluids pour les applications thermiques, Technique de l'ingénieur : nm5115.
[22] Golkonda, V. A and Srinivasa, K.R. (2019), CFD Analysis of a Double Pipe Heat Exchanger by using Fluid Based Nanomaterials, International Journal of Trend in Scientific Research and Development (IJTSRD), Volume: 3 | Issue: 2 | Jan-Feb 2019. www.ijtsrd.com e-ISSN: 2456 - 6470
[23] Arani1, A.A.A S. Khandan, S.S. Ghadimi, B and Sheikhzadeh, G.A.(2014), Numerical investigation of nanofluids swirail floow in circular tube equipped with twisted tape, International Conference on Nuclear and Renewable Energy Resources, Antalya, TURKEY, 26-29 Oct. 2014.
[24] Sai, K. H. Van, T.D and Gerardo, D. (2020), Two-phase flow performance prediction for minichannel solar Collectors, Heat and Mass Transfer (2020) 56:109–120.https://doi.org/10.1007/s00231-019-02686-y
[25] Adrian, B and Allan, D. K. [2003], Heat transfer handbook, Hoboken, John Wiley &Sons, Inc.,New Jersey**.**

[26] Frank M. W.(2009) Fluid Mechanics . (Mc Graw-Hill. New York)**.** ISBN 978-0-07-352934-9

[27] Greg, F. N. and José A. C. (2008), Entropy-Based Design and Analysis of Fluids Engineering Systems, (CRC Press. Taylor & Francis Group Boca Raton London New York).ISBN: 978□0□8493□7262□9

[28] Adrian Bejan (2016), Advanced Engineering Thermodynamics (John Wiley & Sons, Inc. New York). ISBN: 9781119281030

[29] Adrian Bejan. (2013), Convection heat transfer, (John Wiley & Sons, Inc., New York)

[30] Paoletti, S. Rispoli, F and Sciubba, E (1989), Calculation of exergetic losses in compact heat exchanger passages, ASME AES, Vol. 10, No. 2, 1989, pp. 21–29.

[31] Benedetti, P and Sciubba,E (1993), Numerical calculation of the local rate of entropy generation in the flowaround a heated finned tube, ASME HTD,Vol. 266, 1993, pp. 81–91.

[32] Jaeseon, L and Mudawar, I. (2006), Assessment of the effectiveness of nanofluids for single-phase and two-phase heat transfer in micro-channels, Int. J. Heat Mass Transf. 50 (2007) 452–463. DOI:10.1016/j.ijheatmasstransfer. 2006.08.001.

[33] Luchao, S and Guangming, F. (2018), Numerical Simulation of Flow and Heat Transfer Characteristics of CuO-Water Nanofluids in a Flat Tube. Frontiers in Energy Research, Article 57 Volume 6, June 2018, doi: 10.3389/fenrg.2018.00057

[34] Saidu, B. A. Sidik, N. A. C and Siti, N. A. Y.(2020), Measurement of Fluid Flow and HeatTransfer Performance in Rectangular Microchannel using Pure Water and Fe3O4-H2O Nanofluid. Journal of Advanced Research in Applied Mechanics 68, Issue 1 (2020)9-21.https://doi.org/10.37934/aram. 68.1.921

[35] Mohammad, Y. Rozli, A.S.M. Kamaruzzaman, Z S and Abeer, A. S. (2020), Thermal and Hydraulic Performance of CuO/Water Nanofluids: A Review. Micromachines 2020, 11, 416.doi:10.3390/mi11040416

[36] Avinash.K.R, Manishankar .D, Niraimozhi. P, Yogesh.R.J. K,Thiruvenkata. R K (2018). Study of Heat Transfer Characteristics of Al2O3 and CuO Nanofluids in the Tube of a Radiator. IJRAR November2018, Volume 5, Issue 4 www.ijrar.org (E-ISSN 2348-1269, P- ISSN 2349-5138).

[37] Belhadj.A, Bouchenafa.R , Saim.R (2018). Numerical investigation of forced convection of nanofluid in microchannels heat sinks. Journal of Thermal Engineering, Vol. 4, No. 5, pp. 2263-2273 July, 2018

[38] Ghandarali. S, Alireza .A, Hamidreza.E, Mahmoud.A. (2016) Analytical study of parameters affecting entropy generation of nanofluid turbulent flow in channel and micro-channel. Thermal Science · DOI: 10.2298/TSCI151112070S

[39] Krishna. K.P.V Varma, Kishore .P.S, Durga Prasad.P.V.(2017) . Enhancement of Heat Transfer Using Fe3O4 / Water Nanofluid with Varying Cut-Radius Twisted Tape Inserts. International Journal of Applied Engineering Research DOI: 10.37622/IJAER/12.18.2017.7088-7095

[40] Shah, R. K., and London, A. L.(1998), Laminar Flow Forced Convection in Ducts (Advances in Heat Transfer)", Published in 1998 byAcademic Press, New York.

[41] https://www.openfoam.com/documentation/tutorial-guide

[42] Patankar, S., Numerical Heat Transfer and Fluid Flow, McGraw-Hill, New-York,1980.

Appendix

1) Representation of parameter of equation in CFD-Post

Analytic	CFD Post	Analytic	CFD Post	Analytic	CFD Post
$\dot{S}'''_{gen}$	Sg	$\frac{\partial u}{\partial x}$	Dux	$\frac{\partial w}{\partial x}$	Dwx
$\dot{S}'''_{gen,h}$	Sgh	$\frac{\partial u}{\partial y}$	Duy	$\frac{\partial w}{\partial y}$	Dwy
$\dot{S}'''_{gen,f}$	Sgf	$\frac{\partial u}{\partial z}$	Duz	$\frac{\partial w}{\partial z}$	Dwz
$\frac{\partial T}{\partial x}$	DTx	$\frac{\partial v}{\partial x}$	Dvx		
$\frac{\partial T}{\partial y}$	DTy	$\frac{\partial v}{\partial y}$	Dvy		
$\frac{\partial T}{\partial z}$	DTz	$\frac{\partial v}{\partial z}$	Dvz		

2) Representation of equation in CFD-Post

Analytic	Expression in CFD Post
$\dot{S}'''_{gen} = \dot{S}'''_{gen,h} + \dot{S}'''_{gen,f}$	Sg = Sgh + Sgf
$\dot{S}'''_{gen,h} = \frac{k}{T^2}\left(\left(\frac{\partial T}{\partial x}\right)^2 + \left(\frac{\partial T}{\partial y}\right)^2 + \left(\frac{\partial T}{\partial z}\right)^2\right)$	Sgh=(k/T^2)*(DTx^2+ DTy^2 + DTz^2)
$\dot{S}'''_{gen,f} = \frac{\mu_{nf}}{T}\left[2\left(\left(\frac{\partial u}{\partial x}\right)^2 + \left(\frac{\partial v}{\partial y}\right)^2 + \left(\frac{\partial w}{\partial z}\right)^2\right) + \left(\frac{\partial u}{\partial y} + \frac{\partial v}{\partial x}\right)^2 + \left(\frac{\partial u}{\partial z} + \frac{\partial w}{\partial x}\right)^2 + \left(\frac{\partial w}{\partial y} + \frac{\partial v}{\partial z}\right)^2\right]$	Sgf = (Muf/T)(2*(Dux^2+Dvy^2+Dwz^2) + (Duy+Dvy)^2 + (Duz+Dwx)^2 + (Dwy+Dvz)^2)

3) expression of gradient of Temperature and velocity and integral in CFD Post is

Temperature Gradient along the x, y and z axes

DTx = maxVal(Temperature.Gradient X)@radial 1

DTy = maxVal(Temperature.Gradient Y)@radial 1

DTy = maxVal(Temperature.Gradient Z)@radial 1

radial 1: Represent location

Velocity (u,v,w) Gradient along the x, y and z axes

Velocity u Gradient

Dux = maxVal(Velocity u.Gradient X)@radial 1

Duy = maxVal(Velocity u.Gradient Y)@radial 1
Duz = maxVal(Velocity u.Gradient Z)@radial 1

Velocity v Gradient
Dvx = maxVal(Velocity v.Gradient X)@radial 1
Dvy = maxVal(Velocity v.Gradient Y)@radial 1
Dvz = maxVal(Velocity v.Gradient Z)@radial 1

Velocity w Gradient
Dwx = maxVal(Velocity w.Gradient X)@radial 1
Dwy = maxVal(Velocity w.Gradient Y)@radial 1
Dwz = maxVal(Velocity w.Gradient Z)@radial 1

Muf is the dynamic viscosity of the fluid

4) Expression for calculation average temperature

- Analytic expression

$$\mathbf{T_m} = \frac{\int_0^R \boldsymbol{uT(2\pi r)dr}}{\int_0^R \boldsymbol{u(2\pi r)dr}} = \frac{\int_0^R \boldsymbol{uTdr}}{\int_0^R \boldsymbol{udr}}$$

- CFD-Poat Expression

$\boldsymbol{T = Tm}$ = *lengthInt((Velocity w)*Temperature)@radial 1 /lengthInt(Velocity w)@radial 1*